APPLICABILITY OF SUB-MODELLING TECHNIQUE FOR DYNAMIC ANALYSIS OF CONCRETE STRUCTURES WITH ATTACHED EQUIPMENT UNDER MISSILE IMPACT

Genadijs Sagals[1], Nebojsa Orbovic[2], and Thambiayah Nitheanandan[3]

[1]Technical Specialist, Canadian Nuclear Safety Commission (CNSC), Ottawa, ON, Canada
(genadijs.sagals@cnsc-ccsn.gc.ca)
[2] Technical Specialist, CNSC, Ottawa, ON, Canada (deceased)
[3] Director, CNSC, Ottawa, ON, Canada

ABSTRACT

This paper describes the work conducted by the Canadian Nuclear Safety Commission (CNSC) related to the numerical simulations of reinforced concrete (RC) structures under deformable missile impact. The current paper is a continuation of the work conducted in the frame of the OECD/NEA[*] IRIS (Improving Robustness Assessment Methodologies for Structures Impacted by Missiles) Phase 3 benchmark project.

The concrete mock-up with two simple structures attached, one welded and another bolted, was built and tested at the VTT Technical Research Centre in Espoo, Finland. This mock-up was impacted by three subsequent missiles with varying velocities in order to obtain the damage accumulation. To examine vibration transmission through the mock-up, the simple structures modelling equipment were attached to the rear wall of the structure, while the missile impact was at the centre of the front wall. The parameters of the missiles and the RC structure were selected to ensure a flexible behavior of the RC target in the impact area with only moderate damages, specifically cracking and permanent deformation without perforation.

The non-linear dynamic behavior of the reinforced concrete slabs under missile impact was analyzed using the commercial FE code LS-DYNA. A hybrid FE model using both 3-D solid and 2-D shell FE models was developed for the target discretization. Since the ultimate objective of this work is to model the entire structure over long time periods, a simplified combined shell-solid model with distributed (smeared) reinforcement was selected and validated. This model employs solid FE around an impact area and shell FE for the rest of the mock-up.

Detailed modelling of a large RC structure with all equipment attached leads to a very large finite element (FE) model. Therefore, two-level FE modelling using sub-modelling approach was employed: first, analyze the vibrations of a reinforced concrete structure with simplified equipment modelling, and second, analyze in detail the equipment connected to it. This approach assumes uncoupled dynamic behavior of the structure and the equipment. While the sub-modelling technique is commonly used in static analysis, a special sensitivity analysis was conducted to prove the applicability of sub-modelling for impact analysis.

INTRODUCTION

Modern Canadian and International design codes and regulatory documents for Nuclear Power Plants require design against impact of externally or internally generated missiles on safety related concrete

structures. This requirement stimulated a large amount of analytical and experimental work conducted in different countries. Based on publicly available data from tests (Nachtsheim and Stangenberg (1981) and Vepsä et al. (2011)), two simulation workshops IRIS_2010 and IRIS_2012 were conducted (Berthaud et al. (2011) and Orbovic et al. (2015)). The authors of the current paper actively participated in both workshops and developed an adequate FE model (Sagals et al. (2011) and Orbovic, Sagals et al. (2015)) that was capable of predicting the main characteristics of post-impact state of a concrete slab, such as perforation velocity, size and shape of damaged area, crack patterns, etc.

The impact-induced vibrations were, however, not addressed in previous studies. No tests have been conducted to examine impact induced vibrations and their propagation through a reinforced concrete structure. Therefore, it was decided to conduct the new international simulation workshop IRIS Phase 3 in the framework of the OECD/NEA, with the main objective to analyze the transmission of the impact induced vibrations through a reinforced concrete structure from the impacted wall to the floors and walls of the structure which are outside the impacted area. The description of the experimental set-up and selection of output variables were provided by Hervé-Secourgeon and Galan (2016). The results of FEA were provided by workshop participants in numerous papers. See, for example, Ezeberry et al., Khasragh et al. and Borgerhoff et al. (2019)

The authors believe that adequate detailed modelling of missile impact on a nuclear containment building with all attached structures, is impractical due to its complexity. Therefore, the sub-modelling technique is proposed to speed up the analysis as described in the next sections. This technique is well established and commonly used for static analysis. However, only a few papers exist showing application of sub-modelling for dynamic impact analysis, see Link et al. (2016) and Singh et al. (2017)). In the earlier work (Sagals et. al (2019)) authors started implementing sub-modelling approach using IRIS Phase 3 mock-up as an example. The current paper is further continuation of this approach.

The main difference between static and dynamic analysis is that in static analysis cut boundary (interface) displacements fully represent sub-model behaviour. In dynamic analysis cut boundary velocities and accelerations are also needed. Commercial explicit code LS-DYNA (2015) used in the paper has the ability to save only cut boundary displacements during the analysis of the full model and then apply them as boundary conditions for subsequent sub-model analysis. Therefore, the main objective for this paper was to verify the applicability of sub-modelling technique and justify the selection of adequate sub-model for the mock-up impacted by three consecutive missiles as shown in Fig. 1. Additionally, FE predictions were compared with test results for some output parameters.

FE MODELLING

As mentioned in Introduction, the description of the experimental set-up and details of FE modelling of IRIS Phase 3 mock-up are provided in referenced papers and in the earlier work by Sagals et. al (2019). Therefore, only a very condensed description of the mock-up model is provided below following by the description of sub-modelling technique first presented by Sagals et. al (2019). All material parameters are also provided by Sagals et. al (2019).

FE Model of the concrete mock-up

Figure 2 shows the new hybrid solid/shell model developed for the mock-up. It was assumed that attached pseudo-equipment will not significantly influence the mock-up behavior. In this case, only one half of the entire model with simplified welded "equipment" could be analyzed first.

The following additional assumptions were made:

- Detailed models of both welded and bolted "equipment" were analyzed separately after obtaining the entire system behaviour (sub-modelling technique). The selection of these sub-models is described below
- Hybrid shell/solid FE mesh with solid 3-D FE around the impact area of the front wall and shell FE for the missile and the remaining part of the mock-up were selected
- 2-D Belytschko-Tsay 4-noded shell FE was used for mock-up and missile modelling, except the front wall around the impact area. 3-D solid 8-noded FE with constant stress was used in this area
- The connection between solid and shell FE was modeled using command CONSTRAINED_SHELL_TO_ SOLID that aligns brick nodes lying along the tangent vector to the nodal fiber, see Fig. 2
- Simplified pseudo-equipment (welded) was modeled using four 3-D Belytschko-Schwer resultant beams and rigid cylinder
- Each attached leg was modelled as a set of equivalent springs connected to the mock-up floor and ground.

Loading sequence:
- 3 missiles were defined for subsequent impacts with impact velocities 91.8, 93.5 and 167 m/s
- 1000 ms simulation time was selected for each impact with additional 200 ms between impacts for relaxation of induced vibrations before the next impact.

Damping:
- Rayleigh damping $C=\square*M+\square*K$ was applied to concrete parts and pseudo-equipment as described by Sagals et. al (2019).
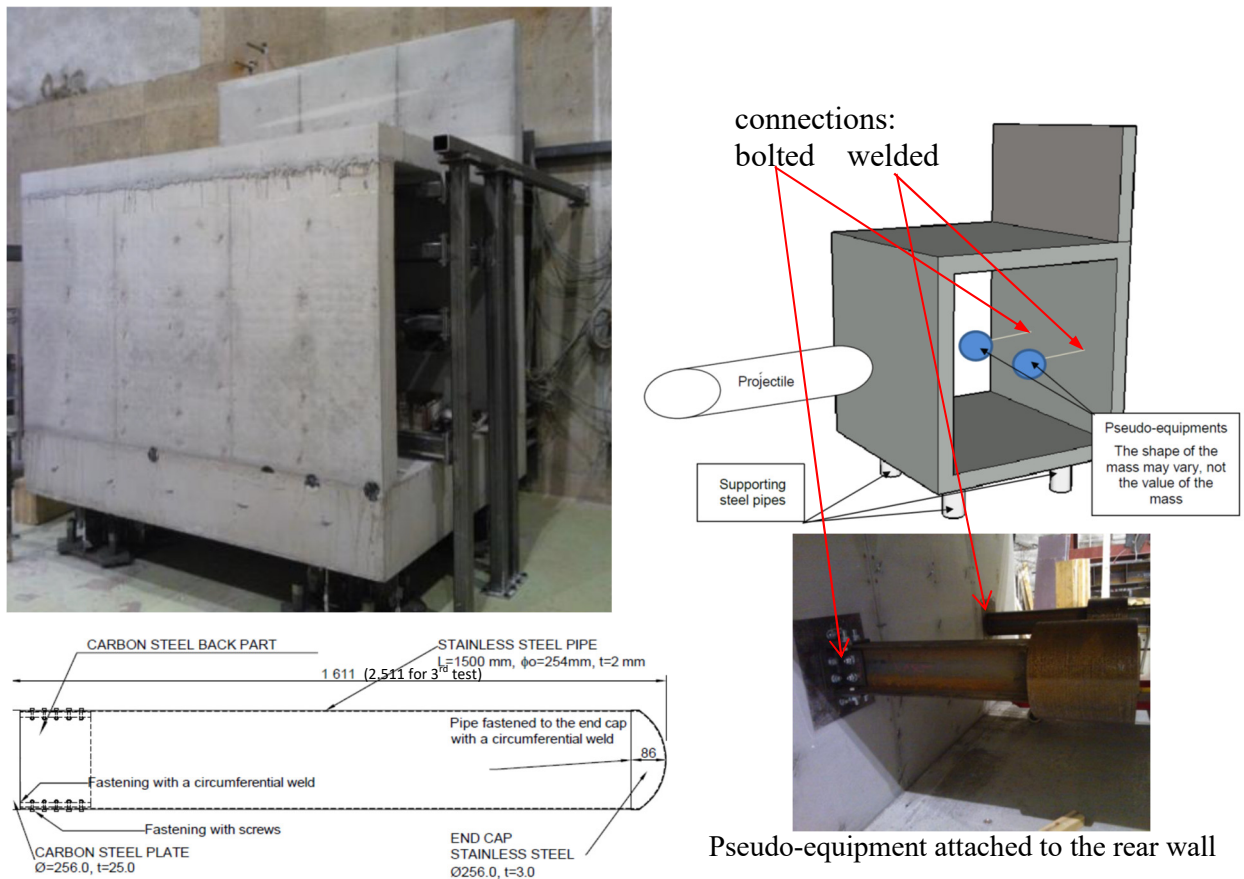

Figure 1. Concrete mock-up and missiles used in IRIS Phase 3 tests

During the analysis of the half of the entire model on Fig. 2 all nodal displacements at the selected sub-model interface were saved for the subsequent detailed modelling of the pseudo-equipment using LS-DYNA command *INTERFACE_LINKING_NODE_SET. After finishing the analysis, saved interface displacements were applied as BC to interface nodes for the newly developed detailed sub-models for both welded and bolted pseudo-equipment as shown in Fig. 3. Separate runs were conducted for each sub-model.
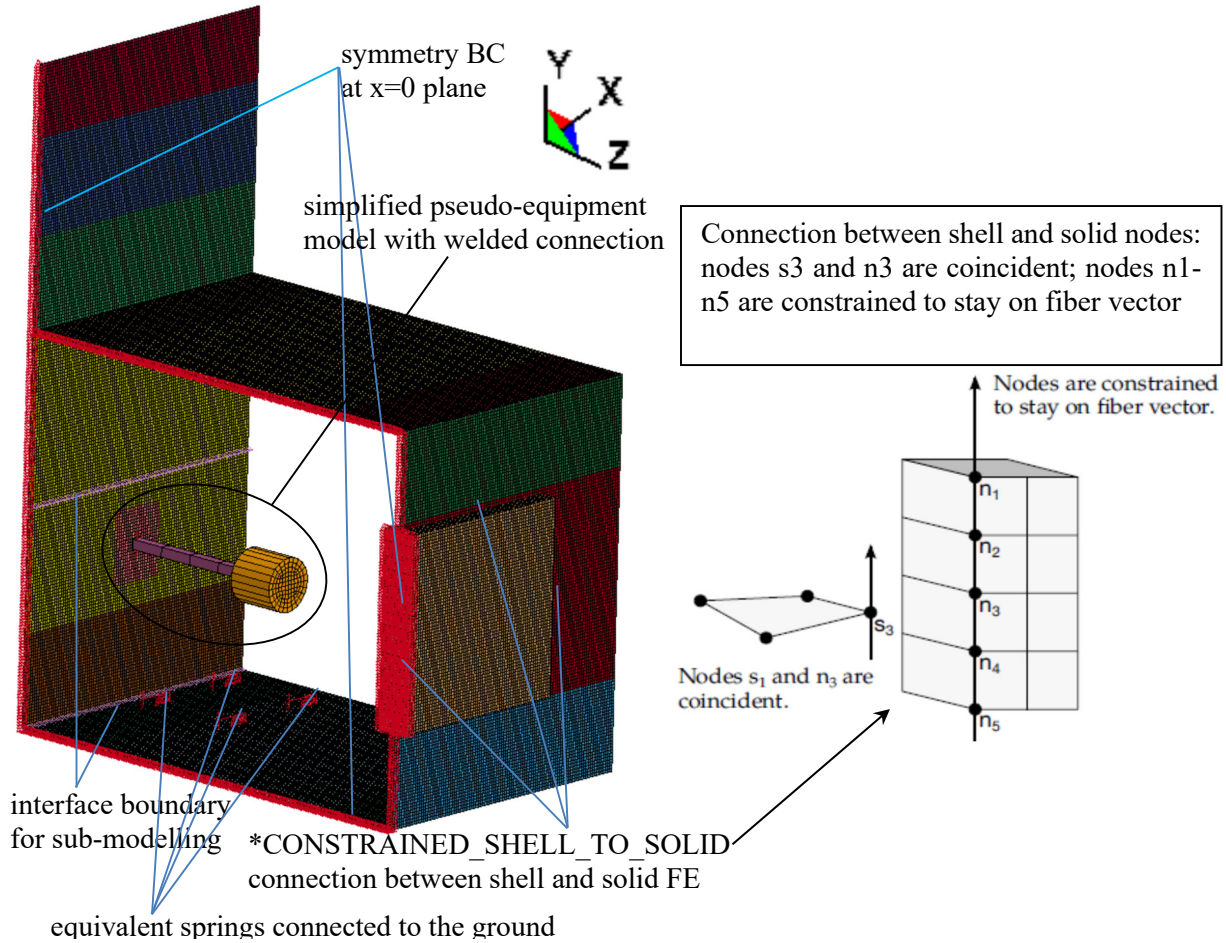
symmetry BC
at x=0 plane

simplified pseudo-equipment
model with welded connection

Connection between shell and solid nodes:
nodes s3 and n3 are coincident; nodes n1-n5 are constrained to stay on fiber vector

Nodes are constrained
to stay on fiber vector.

n_1

n_2

n_3

n_4

s_3

Nodes s_1 and n_3 are
coincident.

n_5

interface boundary
for sub-modelling

*CONSTRAINED_SHELL_TO_SOLID
connection between shell and solid FE

equivalent springs connected to the ground

Figure 2. ½ of the entire mock-up model with selected interface boundaries and simplified welded pseudo-equipment

MODELLING RESULTS

Modelling results were arranged into two groups as follows: (i) verification of the applicability of sub-modelling and selection of the appropriate sub-model, and (iii) comparison of FE predictions for selected output variables with test results.

Selection of the appropriate sub-model

Sensitivity analysis was conducted to select an adequate sub-model that was used for detailed analysis of pseudo-equipment. Three different sub-models: "large" (Fig. 3), "medium" (Fig. 4(a)) and "small" (Fig. 4(b)) were selected during the first analysis of the one half of the entire model. All these sub-models have the same model of attached pseudo-equipment. The difference is in the included area of the back wall as follows:
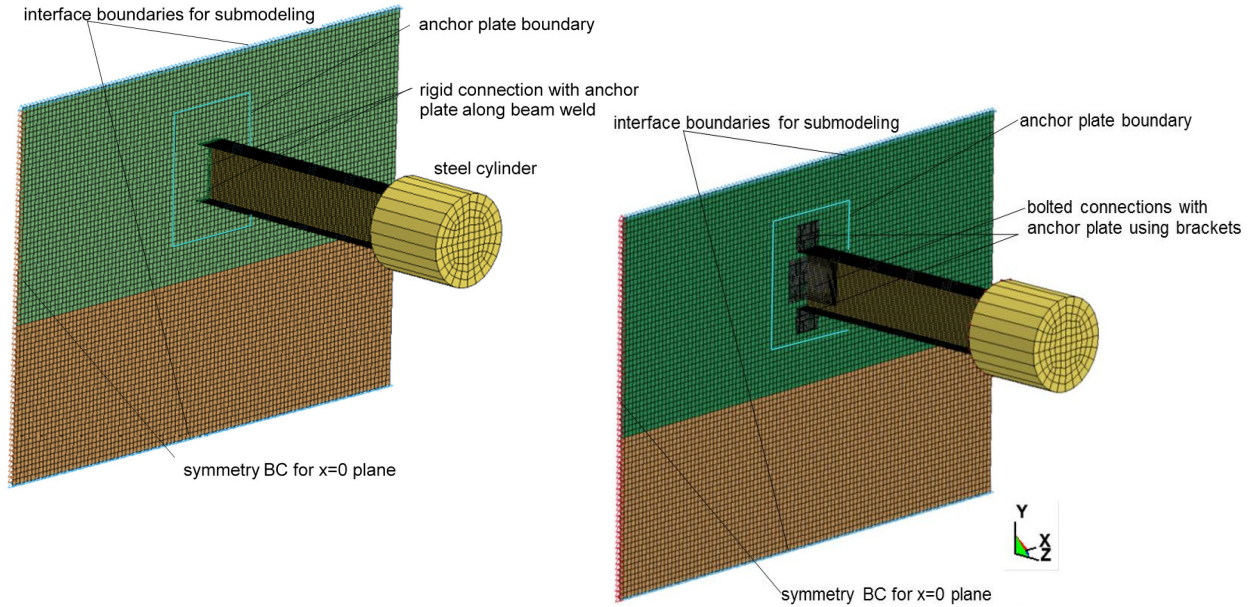
Figure 3. Detailed models of attached pseudo-equipment used in FEA

- 250mm×350mm area of the back wall is included in the "small" sub-model. This area includes only pseudo-equipment anchor plate and underlying concrete wall,
- 350mm×450mm area of the back wall is included in the "medium" sub-model. This area includes also strips of concrete wall around pseudo-equipment anchor plate, and
- 1250mm×888mm area of the back wall is included in the "large" sub-model. This area covers the entire width of the ½ of back wall.

Separate runs were conducted for each sub-model of welded or bolted pseudo-equipment. To decrease modelling time, only 200 ms were modeled for each impact following by 200 ms of relaxation. Therefore, the total modelling time was 1200 ms instead of 3600 ms used in the next section for comparison with test results.

The welded sub-model is much 'stiffer" than bolted and, therefore, represent the bounding case for sub-modelling analysis. For this reason, only welded sub-model was examined in this subsection.
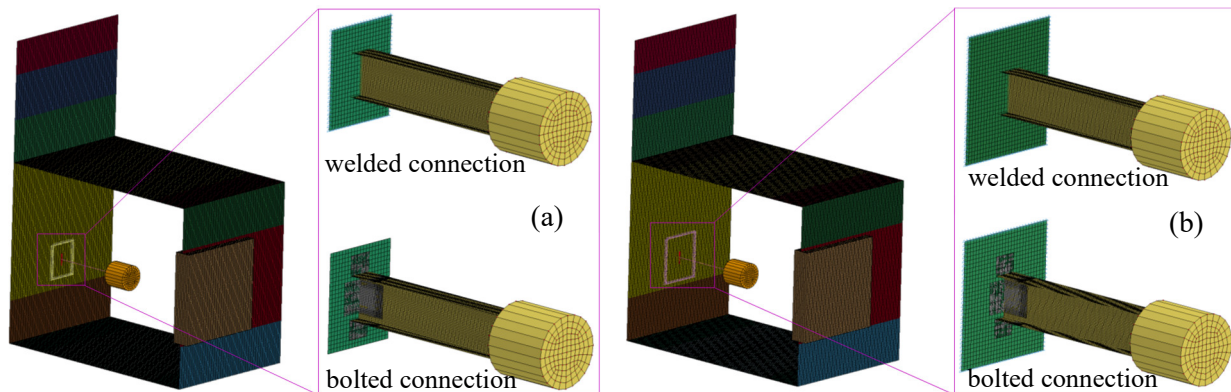

Figure 4. "Small" (a) and "medium" (b) sub-models of attached pseudo-equipment

Test runs conducted show that cut boundary displacements should be saved at each time step during analysis of the full model. Omitting saving at some time steps and using interpolation instead could result in wrong values of cut boundary velocities and accelerations since they are not directly transmitted from the full model. Fortunately, this fact does not lead to a significant increase in analysis time and disk space requirements for the sub-model boundary with reasonable number of nodes.

Fig. 5 shows horizontal (x and z) and vertical (y) displacements at the center of steel cylinder for all selected sub-models. The results clearly show "abnormal" behavior of horizontal displacements of the "small" sub-model during the third impact. Both "medium" and "large" sub-models show similar behavior for the selected outputs during all three impacts with some small differences between them. FE predictions for these sub-models are also similar to the predictions for the entire model. However, the analysis of the additional outputs shows that the "large" sub-model yields better results and, therefore, was selected for both welded and bolted pseudo-equipment.
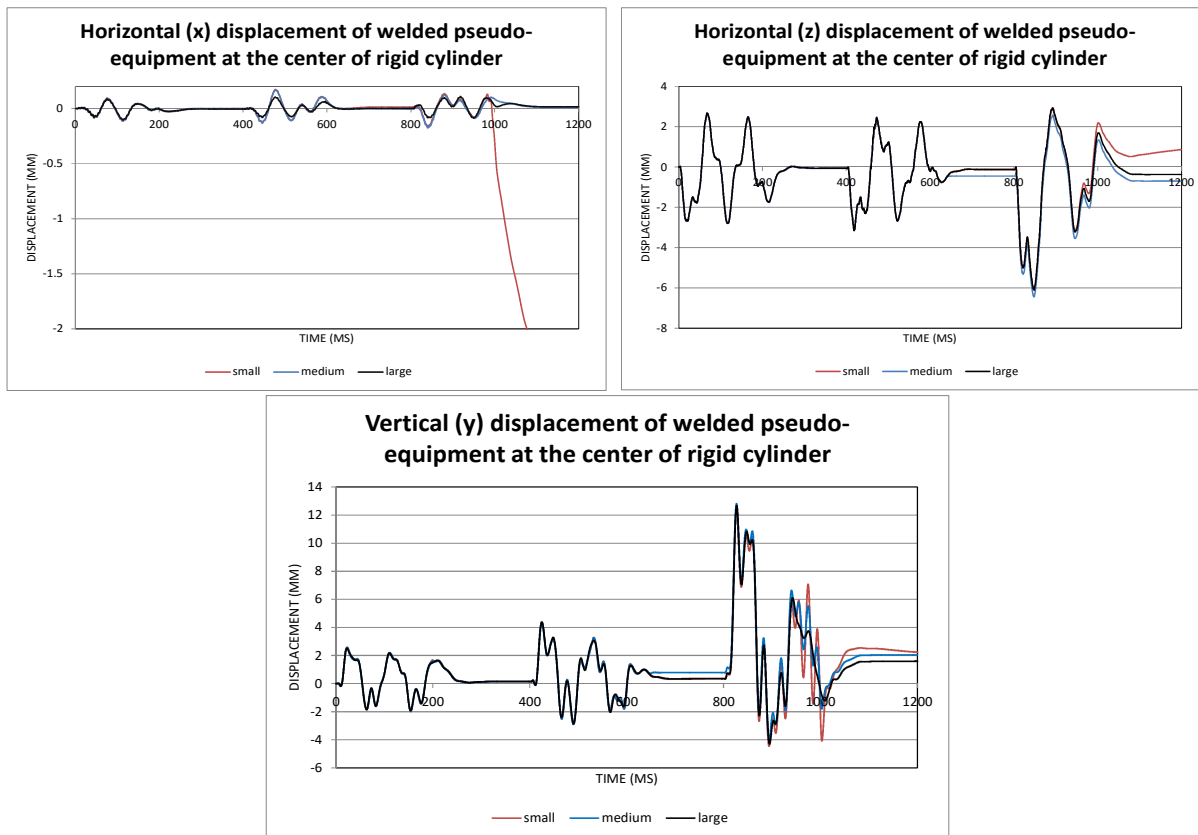

Figure 5. Horizontal (x and z) and vertical (y) displacements at the center of steel cylinder for all selected sub-models

To verify the accuracy of sub-modelling technique, additional analysis was conducted using the "large" sub-model with the largest back wall area and the same simplified equipment model that was used in full model, see Fig. 6. In static analysis this model should produce results identical to the full model. However, as stated earlier, this could be not the case for dynamic analysis. Fig. 6 shows horizontal (x and z) and vertical (y) displacements at the center of steel cylinder for selected sub-model and full model respectively. The results clearly show the almost identical displacements for both models.

Next Fig. 7 shows vertical (y) accelerations for both models. Due to large high-frequency oscillations it is difficult to do comparison in time domain. Therefore, response spectra were calculated

from LS-DYNA output accelerations using ANSYS post-processor, see Fig. 7. The first bending modes for the cantilever beam are approximately 17, 37 and 55 Hz around y-, z- and x- axes respectively. Therefore, 400 Hz was selected as cut-off frequency in Fig. 7. As expected, the difference for accelerations is larger than for displacements. However, sub-modelling technique provide the adequate degree of accuracy also for sub-model accelerations in the selected frequency range.
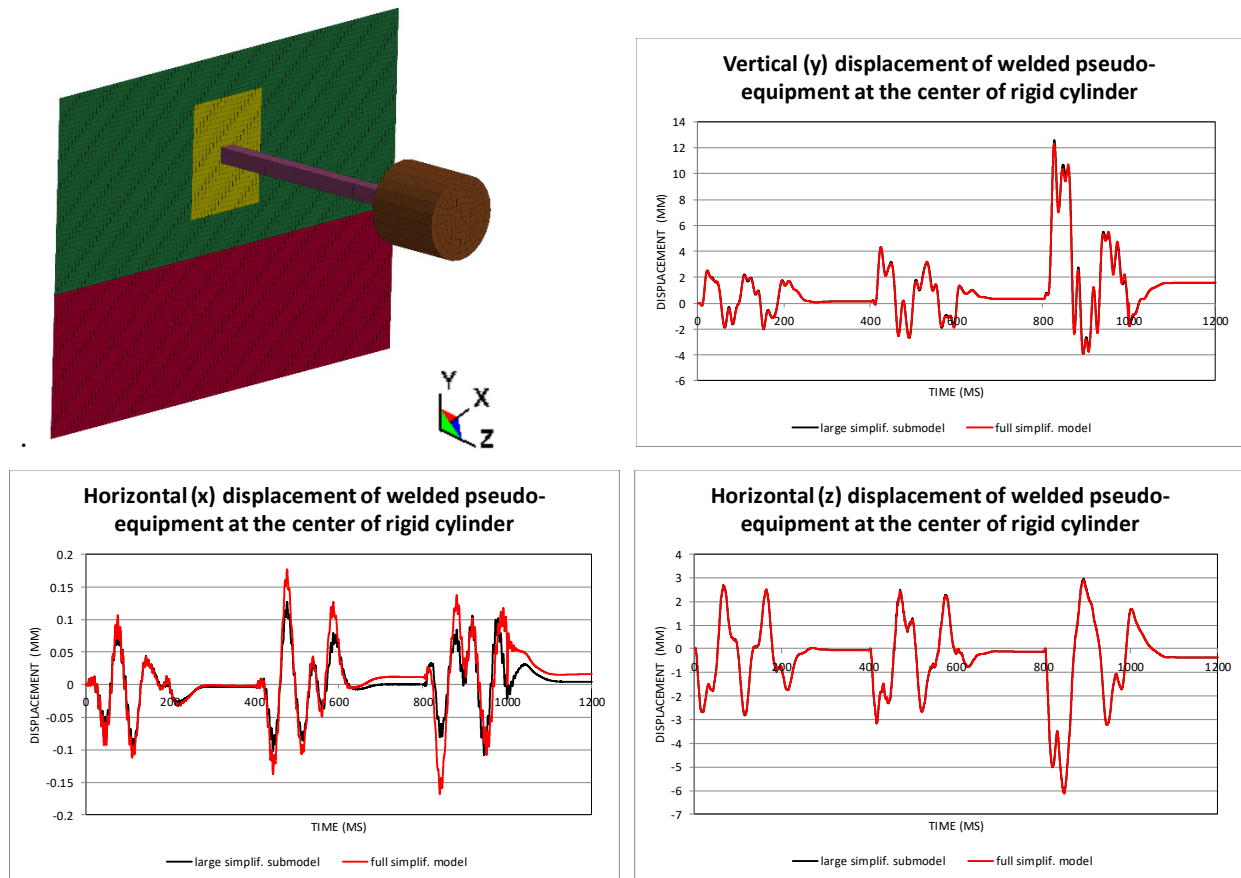

Figure 6. Displacements at the center of steel cylinder for "large" sub-model and full model with identical simplified welded equipment model
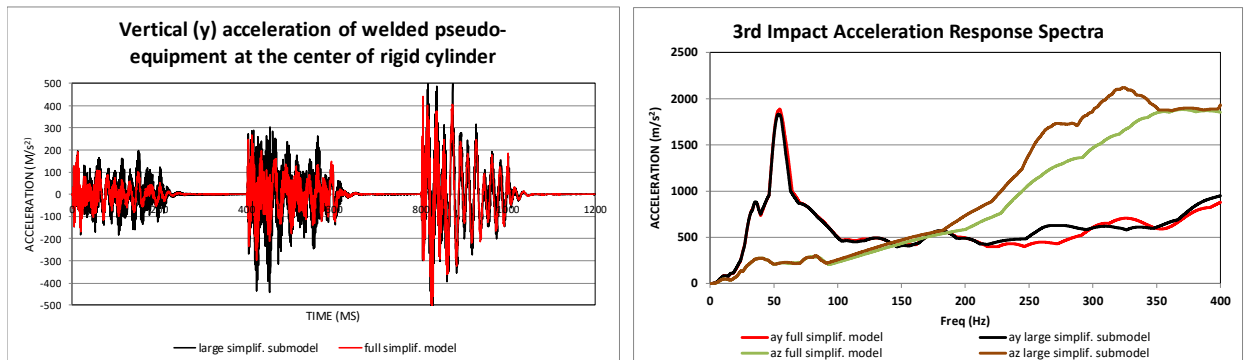

Figure 7. Vertical accelerations and response spectra at the center of steel cylinder for "large" sub-model and full model with identical simplified welded equipment model

Mock-up Results

Figure 8 shows predicted and test displacements D10'=D10w (welded) and D10=D10b (bolted) after the first impact at sensor locations (center of steel cylinder). These vertical displacements were calculated using both the full model (with simplified welded pseudo-equipment) and detailed sub-models. As expected, bolted connection leads to increased vertical displacements. No significant difference was observed between predictions for the simplified and detailed models of welded pseudo-equipment. As expected, the difference between the simplified welded and detailed bolted models of pseudo-equipment is much more pronounced.
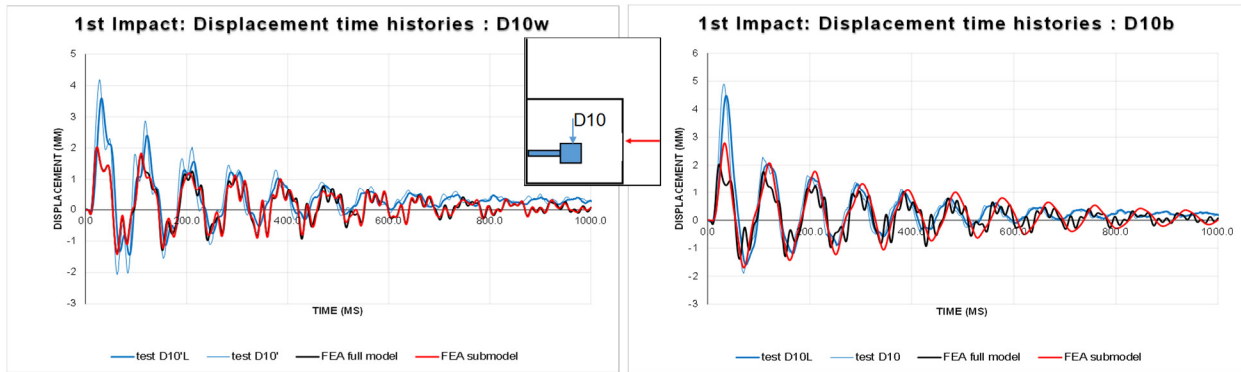

Figure 8. Vertical (y) displacements D10w (welded) and D10b (bolted) after the first impact

Pseudo-equipment displacements after the second missile impact are similar to the displacements after the first impact with slightly higher amplitudes and, therefore are not discussed in this paper. Finally, Fig. 9 shows predicted and test displacements D10'=D10w (welded) and D10=D10b (bolted) at sensor locations during the last (third) impact. As expected, bolted connection again leads to increased vertical displacements. Larger difference was observed between predictions for the simplified and detailed models of welded pseudo-equipment. FE predictions using the detailed model are generally closer to test results.
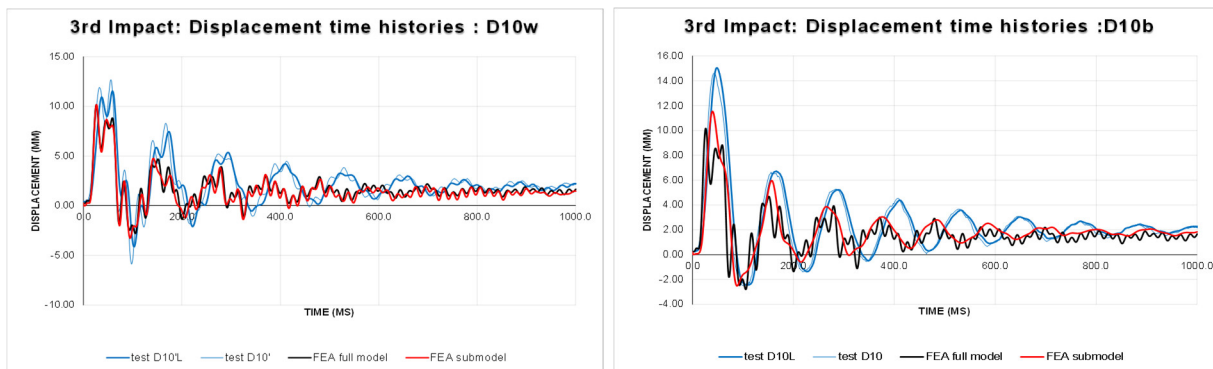

Figure 9. Vertical (y) displacement D10w (welded) and D10b (bolted) after the last (third) impact.

Next Fig. 10 shows predicted and test accelerations of welded and bolted pseudo-equipment. Due to large high-frequency oscillations it is difficult to do comparison in time domain. Therefore, response spectra were calculated similar to previous section, see Fig. 11. The results show some significant differences caused by high-frequency oscillations for the bolted connection. Therefore, some mitigation measures were applied as follows: (a) use for sub-model time step equal or smaller than for the entire mode, and (b) use averaging/filtering for sub-model results, particularly acceleration.
Fig. 11 also shows filtered accelerations using moving 5-points averaging. Significantly better results were
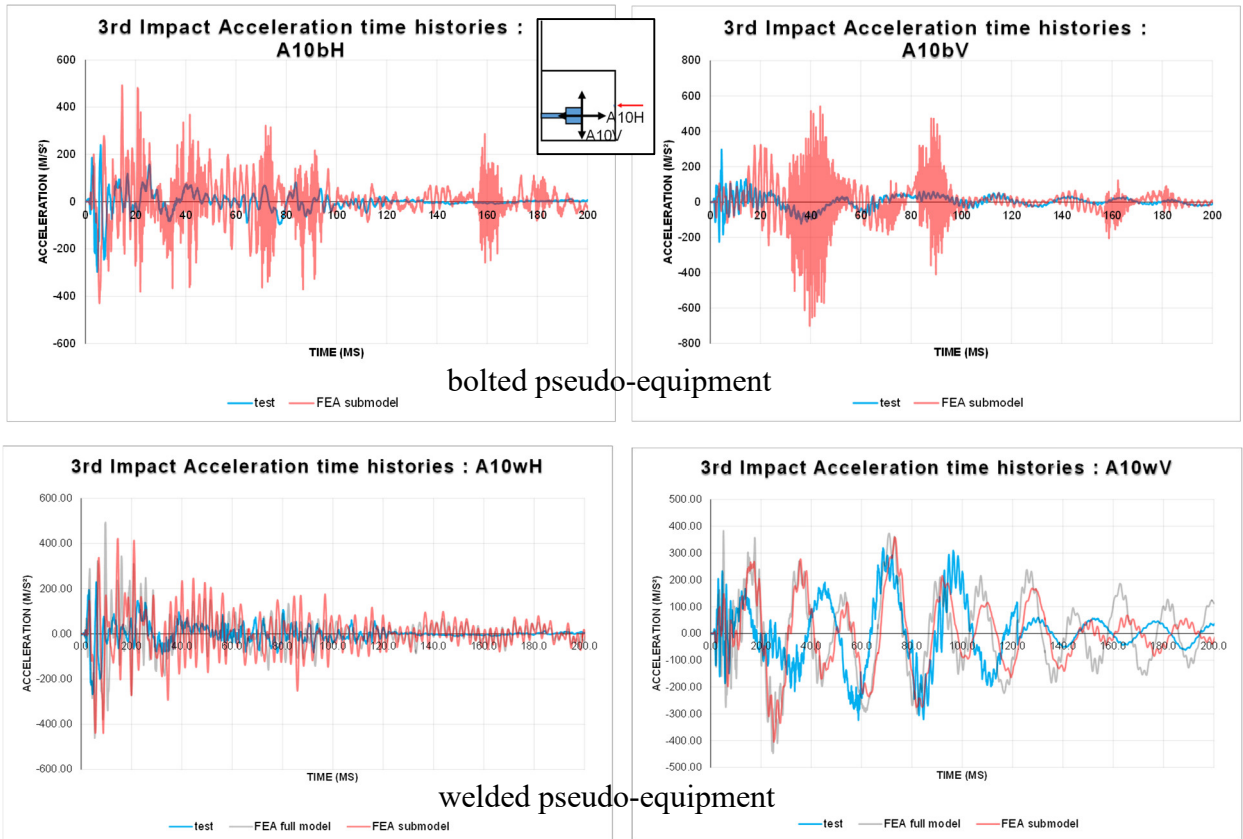
bolted pseudo-equipment

welded pseudo-equipment

Figure 10. Vertical (y) A10*V and horizontal (z) A10*H accelerations after the last (third) impact

bolted pseudo-equipment
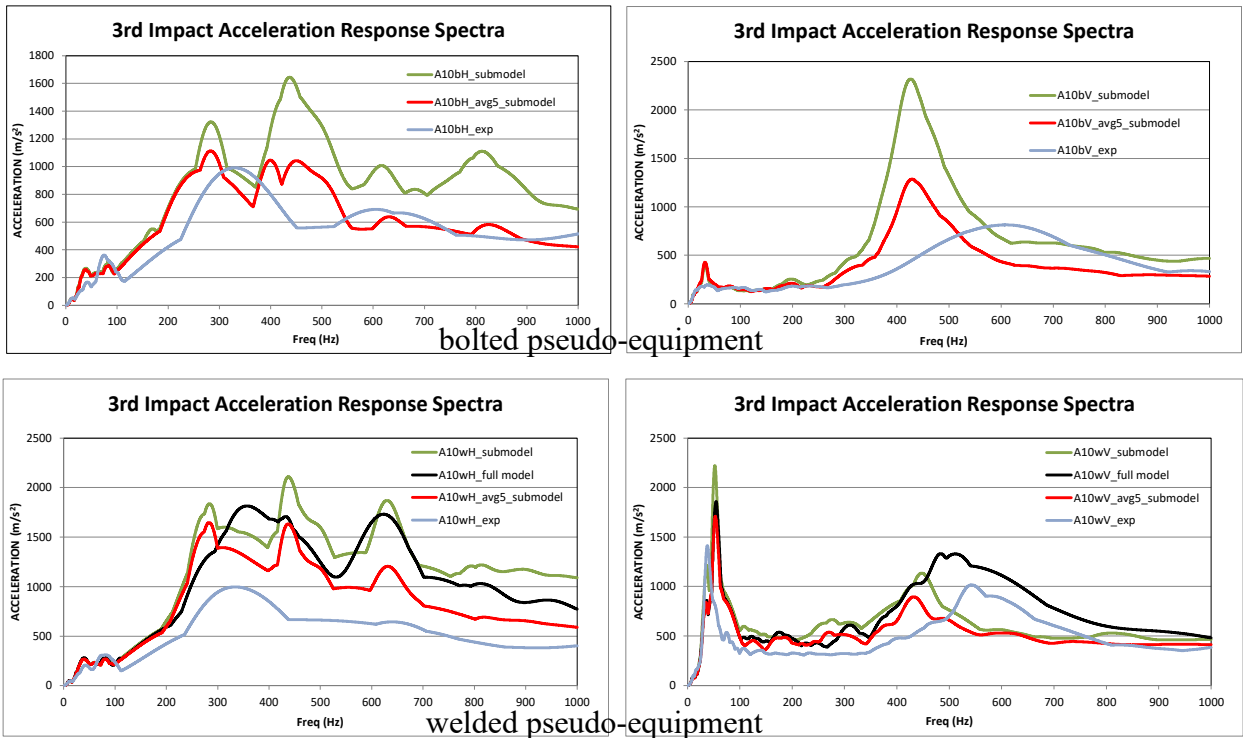
welded pseudo-equipment

Figure 11. Horizontal (z) A10*H and vertical (y) A10*V accelerations response spectra after the last (third) impact for the bolted and welded pseudo-equipment. *_exp – test results

obtained using this simple filter. Some residual high-frequency oscillations still exist for bolted connection, probably caused by numerical instabilities in contact interfaces representing these connections. However, the frequency range of these oscillations is outside the range of equipment dominant frequencies. It is expected that for real containment dynamic behavior of the structure and the equipment is more uncoupled and, therefore, the results should be better than for mock-up.

CONCLUSIONS

The FE model developed using hybrid shell/solid FE and sub-modelling technique produces reasonable displacements at sensor locations for both bolted and welded pseudo-equipment.
Sub-modelling allows a significant reduction of analysis time for the non-linear analysis of components inside real containment in time domain. Additionally, the sensitivity analysis or optimization of these components could be conducted using much smaller sub-models.
However, Sub-modeling could produce significant unwanted high-frequency oscillations of acceleration at sensor locations. Mitigation measures were proposed to mitigate these oscillations as follows:
- Use for sub-model time step equal or smaller than for the entire mode
- Use averaging/filtering for sub-model results, particularly acceleration

REFERENCES

Berthaud Y., Benboudjema F., Colliat J.-B., Tarallo F., Orbovic N. and Rambach J.-M. (2011). "IRIS_2010 - Part IV: Numerical Simulations of Flexural VTT-IRSN Tests," *Transactions of the SMiRT 21*, pp 855-862, New Delhi, India.

Borgerhoff M., Riesner F., Schneeberger C., Stangenberg F. and Zinn R. (2019). "Impact induced vibrations of reinforced concrete structures determined by linear and nonlinear analyses of tests performed within Impact III project," *Transactions of the SMiRT 25*, Charlotte, NC, USA.

Ezeberry J., Combescure D. and Ayneto J. (2019). "Impact assessment of ITER RC structures - 3rd phase of the OCDE-IRIS benchmark," *Transactions of the SMiRT 25*, Charlotte, NC, USA.

Hervé-Secourgeon G., Galan M. and Darraba A. (2016). "IRIS Phase 3 - Description of IRIS Phase 3 Project," Tech. Report, Électricité de France, https://www.researchgate.net/publication/318129906.

Khasraghy S. G., Karbassi A., Schneeberger C. and Zwicky P. (2019). "Vibration propagation of reinforced concrete structures under consecutive impacts," *Transactions of the SMiRT 25*, Charlotte, NC, USA.

Link S., Singh H., and Schumacher A. (2016). "Influence of submodel size and evaluated functions on the optimization process of crashworthiness structures," LS-DYNA Forum, Bamberg, Germany.

LS-DYNA® R8.0 User's Manual (2015), Livermore Software Technology Corp.

Nachtsheim, W. and Stangenberg F. (1981). "Impact of deformable missiles on reinforced concrete plates-comparisonal calculations of Meppen tests," *Transactions of the 6th SMiRT*, Paris, France.

Orbovic N., Tarallo F., Rambach J.-M., Sagals G. and Blahoianu A. (2015). "IRIS_2012 OECD/NEA/CSNI benchmark: Numerical simulations of structural impact," *Nucl. Eng. and Design*, 295, pp. 700–715.

Orbovic N., Sagals G. and Blahoianu A. (2015). "Influence of transverse reinforcement on perforation resistance of reinforced concrete slabs under hard missile impact," *Nucl. Eng. and Design*, 295, pp. 716–729.

Sagals G., Orbovic N. and Blahoianu A. (2011). "Sensitivity Studies of Reinforced Concrete Slabs under Impact Loading," *Transactions of the SMiRT 21*, pp. 783-791, New Delhi, India.

Sagals G., Orbovic N., and Nitheanandan T. (2019). "FE analysis of reinforced concrete structures under missile impact using sub-modelling technique" *Transactions of the SMiRT 25*, Charlotte, NC, USA.

Singh H., Schumacher A., Falconi C., Walser A., Trentmann S., Benito L., Foussette C. and Krause P. (2017). "Hierarchical Multi-Level-Optimization of crashworthy structures using automatic generated submodels," 11th European LS-DYNA Conference, Salzburg, Austria.

Vepsä, A. et al. (2011). "IRIS_2010 - Part II: Experimental Data," *Transactions of the SMiRT 21*, pp. 2519-2527, New Delhi, India.